RESEARCH ARTICLE OPEN ACCESS

Yield and Particle Morphology of Spray Dried Salts: Fractional Factorial Design

Abanti Sahoo[1] and Arati Parihari[2]
[1, 2] *Chemical Engineering Department, National Institute of Technology, Rourkela-769008, India.*

ABSTRACT
The yield of the spray drier has been correlated with the various system parameters namely inlet temperature, aspirator speed, feed flow rate, salt-concentration, atomization rate and molecular weight of salt on the basis of dimensional analysis approach. Attempt has also been taken to design the experiments by Fractional Factorial Design method for both cases i.e. for the blank solution (water) and for the salt solution. The results thus obtained through these developed correlations (by Dimensional Analysis and Fractional Factorial Design) have been validated with the results obtained by ANN-approach and finally the findings obtained from all the approaches have been compared with the experimentally observed values. Attempt was also made to study the particle morphology through the Scanning Electron Microscope.
Keywords: Yield, Morphology, Regression analysis, Fractional Factorial design, Artificial Neural Network and Scanning electron microscope.

I. INTRODUCTION

Spray drying is the most widely used process for the particle formation and drying in industrial as well as laboratory scale. It is a continuous operation in which almost all pumpable solution can be converted into a free flowing powder. The process involves conversion of fluid into fine droplets thereby exposing them to a hot drying media, so as to achieve defined dry particulate matter [1]. Some advantages of spray drying include the ability to produce a dry powder rapidly and the ability to control the particle size distribution. The limitations of spray drying include problems of efficient particle collection and the potential instability of materials which are sensitive to high temperatures. The primary goal of spray drying is removal of water [2]. Under normal operating conditions the powder-particles should be enough dried before hitting the walls of the spray dryer so that they do not stick to the walls [3]. The drying behavior strongly depends on the spray characteristics and the feed composition. Stickiness is related to the drying state of the particles. Improper operating conditions which do not match the drying behavior of the particles can therefore lead to fouling. The objective of this study is to examine the effects of process variables on particle size and other properties of various spray-dried salt solutions. The effects of various process parameters on the spray-dried product have been examined using a lab-scale apparatus. Prediction of the effects of parameters on particle characteristics is very much useful in optimization of the process for development of spray-dried products.

II. LITERATURE

Maury et al. [4] developed an improved glass cyclone for the laboratory spray drying in an effort to increase yield. The effects of the various parameters (namely, concentration & flow rate of the liquid feed; inlet temperature, outlet temperature, flow rate of drying air and the atomizing air flow rate) on yield of the product and residual moisture content have been studied by many researchers [4,5 &7-17]. In all cases the moisture content of the products is always observed to decrease with increase in compressed air flow rate and the drying air temperature is observed to be the most important factor affecting the solubility. Zhou et al. [5] also studied the effects of parameters on crystal protein content and lethality of product. Zhonghua & Mujumdar [6] dried concentrated common salt (NaCl) solution using spray dryer in the intense oscillating high-temperature turbulent flow field generated in the tail pipe of a pulse combustor. Thus, it was concluded that pulse combustion drying can be applied to drying of fine droplets of highly heat-sensitive materials although the jet temperature is initially extremely high. Chegini & Ghobadian [7] studied the drying of fruit juice in a spray dryer to determine the sticky point-temperature for orange juice powder. Athanasia and Konstantinos [8] investigated the performance of a pilot spray dryer for tomato powder preparation. Phogpipatpong et al. [9] studied spray drying with co-current operation and a two fluid nozzle atomizer. A regression model in the form of second order polynomial was developed which describes the product characteristics with respect to the independent variables. Product yield is observed to increase with increase in drying air temperature and malto-dextrin ratio. However the yield was observed to decrease with increase in air velocity. Prinn et al. [10] examined the effects of formulation and process variables on particle size and other characteristics of a spray-dried model protein. They observed protein concentration to be the determining parameter for the product yield.

Lin & Gentry [12] have observed that the shell structure of a drying droplet plays an important role in determining the morphology of final dried particle. Iskandar et al. [13] found that the structural stability of the droplet and the hydrodynamic effects during the drying process play important roles in controlling the morphology of the resulting particles. They also observed that size of the sol in the droplet, droplet size, viscosity of droplet, drying temperature, gas flow rate and addition of surfactant affect the morphology of particles. The appropriate choice of the types of spray dryers with varied operating conditions was also observed to control the particle size and shape ranging from spheres to ellipsoids as well as doughnut-shaped particles. Donhowe et al. [14] characterized the effects of exhaust heat recovery in addition to other parameters on the energy consumption of a concurrent-flow spray dryer. Heat recovery is observed to reduce the energy consumption of the dryer by 12–28%. Kent & McLeod [15] observed that once the dryer inlet temperature, dryer outlet temperature, and other parameters are optimized for a specific product under specific conditions, dryer outlet moisture will be optimized automatically. Greenwald & Judson [16] characterized the effects of the design and operating conditions of spray drying on the morphological behavior of the product. Bhandari et al. [17] developed a semi-empirical linear equation to optimise the amount of malto-dextrin additive (DE 6) required for successful spray drying of a sugar-rich product on the basis of its composition. The drying index values for individual sugars (sucrose, glucose, fructose) and citric acid were determined based on spray drying experiments and using these index values an equation for modeling was also established by them which was found to be satisfactory on testing.

Zbicinski et al. [18] employed advanced experimental techniques (including laser techniques) to determine current parameters of spray drying process (temperature, humidity, moisture content) and current structure of spray (particle size distribution, particle velocities, etc.). It is proved that spray residence time is controlled by atomization ratio and airflow rate. It is also concluded that the generalized drying curve obtained from small-scale experiments could be used to describe spray-drying kinetics if the critical moisture content of the material is known. Katarzyna et al. [19] observed that high feed ratio speed and low outlet air temperature result in highly actived enzyme. Chegini and Ghobadian [20] investigated the effects of the feed ratio, atomizer speed, and inlet air temperature on properties of spray-dried orange juice powders and developed a correlation based on a full factorial experimental design. Namaldi et al. [21] investigated the stabilization of spray drying and subsequent storage problem. It is observed that the presence of additives in most cases provide higher activities both after drying and during storage period compared to no additive case.

Anandharamakrishnan et al. [22] studied the effects of varying feed concentration (20-40% w/v) and outlet temperature (60 to 120°C) on whey protein denaturation (determined by DSC) and solubility (at pH 4.6) using a co-current spray dryer. It was concluded that crust formation resulting in high particle temperatures while still maintaining a wet core is likely to lead to high levels of denaturation.

III. Regression Analysis

In regression analysis modeling is done by analyzing several variables, when the focus is on the relationship between a dependent variable and one or more independent variables. More specifically, regression analysis gives idea about how the typical value of the dependent variable changes when any one of the independent variables is varied, while the other independent variables are held constant. Most commonly, regression analysis estimates the average value of the dependent variable or final output when the independent variables are held constant. Thus the estimation target is a function of the independent variables and is called the **regression function**. In regression analysis, the variation of the dependent variable can be characterized around the regression function, which can be described by a probability distribution. Another common statistic associated with regression analysis is the R^2, coefficient of determination. A high value of R^2, suggests that the regression model explains the variation in the dependent variable well and is obviously important if one wishes to use the model for predictive or forecasting purposes.

In the present work, the correlations for outputs (i.e. yield and outlet temperature) have been developed on the basis of regression analysis. In this approach, one parameter is varied at a time when other parameters are maintained constant. The outputs corresponding to the different values of varied input parameter are measured. Then the noted output values are plotted against the corresponding values of that particular input parameter which is a power curve or whose nature is exponential-type. Similarly effect of all other parameters are analysed and finally all these effects of parameters are combined. Products of all these parameters (where each parameter is raised to its own exponent) are plotted against the output values (power curve) to get the overall exponent and coefficient for the developed correlation.

IV. Design of Experiment – Fractional Factorial Design

Factorial Design or statistical analysis is common in designing experiments for engineering and scientific applications. In many cases, the factors affecting the production process are considered at two levels [23]. Thus the experimenter can determine whether any of these changes affect the results of the production process or not. The most important thing to study these factors will be to vary the factors of interest in a full factorial design, that is, to try all possible combinations of settings.

With two cube, 2^3 Factorial Design, the correlation will be written in the following form.

$$Y_{ijv} = a_0 + a_1 A + a_2 B + a_3 C + a_{12} AB + a_{13} AC + a_{23} BC + a_{123} ABC \quad (1)$$

If more than four factors are involved, the complete factorial might involve more than a practical number of experiments. For example, a 2^5 factorial design would require 32 experiments. By careful selection of the experimental conditions it is possible with only a fraction of the total experiments required for the complete factorial to determine the main effects by aliasing them with the higher order interactions which are usually not significant.

The eight experiments required for a complete three factor, two level factorial can be used to determine the change required in four, five or even in seven experimental variables under ideal conditions to obtain the maximum change in the response variable.

As (n-p) factorial design is set up and the p factors not included in the complete 2^{n-p} factorial, they are aliased with one of the higher order interactions to form a generating contrast.

V. Artificial Neural Network Approach

An ANN-based model has also been defined in literature as a computing system made up of a number of simple and highly interconnected processing elements. This system processes information by its dynamic state response to external inputs as discussed by many authors [24]. The back propagation network is the best known and widely used approach among the current types of neural network systems. The same method has also been used in the present study to find out the percentage of yield and the outlet temperature.

VI. MATERIALS AND METHODS

The experimental unit used in the laboratory is LU222 Advanced Labultima Laboratory Spray Dryer as shown in Fig-1. Four different salts were considered for the experimentation. The various system parameters explained as scope of the experiment are shown in Table-1. These are varied to study their effects on the outlet parameter (i.e % yield of salt and the outlet temperature). After each experiment the output namely the %yield and the outlet temperature are measured. The samples are also collected after every run of the experiment and are processed for the moisture analysis and S.E.M. analysis. The experimentally observed output data are then correlated with the various system parameters on the basis of the conventional dimensional analysis or regression analysis. The calculated output data thus obtained are then processed to predict the output by the statistical analysis (Fractional Factorial Design) and ANN approaches for further validation.

VII. Moisture Analysis

Moisture analysis has been performed on dry samples using an Electronic Moisture Analyzer Model MA150 (temperature range 40 to 200^0C, weighing capacity 159 gm with minimum sample weight 0.1 gm). All spray-dried samples were found to have final moisture content in the range of 0.2% to 1.5% wt/wt irrespective of the parametric conditions maintained in the spray dryer. All samples are stored in sealed vials and physical characterizations have been performed within 24 to 48 hours. No change in the moisture content has been observed at the end of this storage time.

VIII. Study of Morphology using Scanning Electron Microscope

SEM images were obtained for all crystalline salts before and after spray- drying to examine the particle morphology. A scanning electron microscope (JEOL 6480 LV JAPAN) was used for imaging after sputter coating of samples with Au. The Sputter Coater uses an electric field and Argon gas. The sample is then placed in a sample chamber at vacuum. Argon gas and electric field cause an electron to be removed from the argon, making the atoms positively charged. The argon ions are then attracted to a negatively charged gold foil. The argon ions knock gold atoms from the surface of the gold foil. These gold atoms fall and settle into the surface of the sample producing a thin gold coating.

IX. RESULTS AND DISCUSSION

The percentage yield and the outlet temperature after each experiment are determined. These results are tabulated against the corresponding system parameters in Table-2. Attempt has been made to develop correlations using these outputs with the respective input data by different methods. The calculated values of the results for dependent variables, i.e. %yield and the outlet temperature obtained through regression analysis are listed in Table 2 (A) and (B) and the respective correlation plots are shown in Fig.-2(A) and (B).

The final correlations for the percentage yield and the outlet temperature thus developed by the conventional Regression analysis method are as given below.

$$Y = 251.09\left[(T_i)^{-0.15}(U_{asp})^{-0.10}(U_p)^{-0.67}(C_s)^{0.07}(P_{i-air})^{-0.25}(M_s)^{-0.04}\right] \quad \text{----- (2)}$$

Correlation coefficient (R) and coefficient of determination (R^2) for %yield, Y are found to be **0.86003** and **0.73965** respectively.

$$T_o = 2.2032\left[(T_i)^{0.08}(U_{asp})^{0.20}(U_p)^{-0.23}(C_s)^{-0.07}(P_{i-air})^{-0.157}(M_s)^{0.13}\right] \quad \text{--- (3)}$$

Similarly correlation coefficient (R) and coefficient of determination (R^2) for outlet temperature, T_o are determined to be **0.96404** and **0.92938** respectively.

The developed correlations for %yield and outlet temperature by 2^{6-2} fractional factorial design method for different salt solutions are shown below.

$$Y = 62.305 - 4.34A + 5.14B - 2.08C - 2.99D + 1.31E - 0.345F - 0.395AB - 2.56AC - 2.27AD + 2.67BC + 2.07BD - 1.28CD - 0.67ABD - 3.89ACD + 0.18ABCD \quad \text{--(4)}$$

$$T_O = 51.96 - 1.294A - 0.406B - 2.98C - 1.56D + 2.606E - 1.45F + 0.194AB - 2.73AC - 3.18AD - 1.84BC + 0.256BD + 3.58CD + 2.08ABD + 0.76ACD + 0.72ABCD \quad \text{--(5)}$$

Where A = T_i, B = U_{asp}, C = U_p, D = C_s, E = (ABC) = P_{i-air}, F = BCD = M_s.

The effects of 2^{6-2} fractional factorial design are listed in the Table-3. The calculated values of the outlet temperature and %yield by fractional factorial design are shown in Table-4 and Table-5 respectively.

A three layered feed forward Neural Network is considered for this problem. The network is trained for a given set of input and target data sets. These sets were obtained from the experimental observations. The data are scaled down and then the network is exposed to these scaled data sets. The network weights are updated using the Back Propagation algorithm. In this back propagation the network corrects its weights to decrease the observed error. The optimum structure of the ANN obtained for all the data sets are shown in Fig.-3.

Comparison plots for the %yield and the outlet temperature of salt solution against the experimental values calculated by different methods (i.e. regression analysis, fractional factorial design and artificial neural network analysis) are shown in Fig.- 4 (A) and (B). Sample plots for particle morphology through SEM are shown in Fig.5 -8.

It is observed that the salt concentration influences the particle size. The higher the concentration of the salt solution, the larger is the yield (dried particles) which is also more porous. The lower the concentration of the salt solution, the smaller and finer are the dried particles. As observed from Eq.- (1), %yield increases with increase in concentration of the salt solution and decreases with the increase in inlet temperature, aspirator speed, pump flow rate, molecular weight of the salt and atomization rate. But with the outlet temperature effect is opposite. It is observed from Eq.- (2), that the outlet temperature of the dryer decreases with increase in pump flow rate, concentration of the salt solution and atomization rate. But it increases with the increase in inlet temperature, aspirator speed and molecular weight of the salt. The condensation rate in the drying chamber increases with increase in the liquid feed rate, aspirator speed and the atomization rate. Condensation inside the chamber causes a loss in yield as evident from eq.- (1). This is so because the dried particles stick to the chamber walls thereby reducing the yield. Most of the sprays resulted in low yields because of the difficulties in collection of particles in spray drying, particularly when trying to produce small sized/fine particles. Many of the fine particles cannot be recovered in the lab-scale apparatus because they do not efficiently deposit in the cyclone as their low masses cause them to be drawn up into the vacuum. The outlet temperatures are observed to vary within 40°C to 90°C. In case of spray drying it is important that the outlet temperature should be low for temperature-sensitive proteins and peptides to avoid product degradation.

In the present work molecular weight of salt (Ms) has been considered as one variable (factor). But for general modeling consideration of molecular weight is not a good idea rather salt property can be considered as the variable as any number does not correspond to the molecular weight of a salt. In the present case four different salts were considered in the solution form. Thus applications of these correlations as such can be limited for these four salts. Certain modifications or scale up factor can be included with these correlations for applicability to other salts.

The morphologies of the different spray-dried powders were examined by SEM. Various particle morphologies as observed are (I) smooth spheres, (II) collapsed or dimpled particles, (III) particles with a "raisin-like" appearance and (IV) highly crumpled, folded structures. The particle morphology plays a profound role in the aerodynamic properties and performance of aerosol applications. For instance a porous crumpled structure results in a much lower aerodynamic particle diameter in comparison with a dense particle. This is so because when the water in the droplet evaporates, a smaller particle only remains back and when the atomizing air flow rate is high, the drop exiting the nozzle tends to be smaller for which the resulting dried particle will be smaller. Average output of the three sets of testing data through ANN-programming was found out to be 0.354704. Normalisation factor was selected as 180 and thus the final output through ANN-approach was obtained as 63.85 % of Yield. Chi square (ξ^2), standard deviation and mean deviation for the correlations developed by both fractional factorial design and regression analysis are shown in Table-6.

From the comparison plot and Table-6, it is observed that although all the three methods give good approximation with respect to the experimental findings the percentage of yield by fractional factorial design approach is closer to the experimentally observed data as indicated by lower chi-square (ξ^2) value and Fig.-4(A).

From the comparison plot for outlet temperature (Fig-4(B)), it is observed that the calculated values of outlet temperature obtained from dimensional analysis is more closer to the experimental values than those obtained from statistical analysis.

X. CONCLUSION

The present studies reveal that the particle morphologies are affected with the variation of parametric conditions of the dryer and the physical characteristics of the sample solutions are also affected. Agglomeration during spray drying depends on drying air temperature in the atomization zone, pump flow rate and atomization rate. That is why proper care should be taken in food industries for the preparation of infant food, instant food mix etc. for getting the moisture free and unaltered product. It is highly essential to have a good understanding of the effects of the process inputs on the final characteristics of the dried product particles for many reasons. Good knowledge on process would lead to better productivity, low operational costs and improved quality of the final product. These studies with the developed models can have wide applications in food, ceramics, chemical and pharmaceutical industries over a wide range of system parameters. Lower values of chi-square (ξ^2) for the correlations developed by both regression analysis and fractional factorial design further strengthen the findings.

NOMENCLATURE

a,b,c,d,e,f ,n	:	Exponents
Y	:	%Yield
Ti	:	Inlet temperature, ^oC
To	:	Outlet temperature, ^oC
Uasp	:	Aspirator Speed, kg/cm^2
Up	:	Pump flow rate, ml/ min
Piair	:	Atomization rate, kg/cm^2
Cs	:	Concentration of salt, gm/ml
Ms	:	Moleccular weight of salt
K	:	Coefficient of the correlation
$(NH_4)_2SO_4$	:	Ammonium Sulfate
NaCl	:	Sodium Chloride
Na_2SO_4	:	Sodium Sulfate
$C_6H_{14}O_6$	:	Mannitol

REFERENCES

[1] Ruud, E.M.V., Han, S., Maykel, V., Jan, J., Van, H., Erik, S., Gerrald, B. & Peter, D.J. (**2002**). Modelling spray drying processes for dairy products. Lait Dairy-Journal Edp Sciences, v. 82, p. 453–463.

[2] Nath, S. & Satpathy, G. R. (**1998**). A systematic approach of spray drying processes. Drying Technology, v.16, n. 7, p. 1173-1193.

[3] Ozmen, L. & Langrish, T.A.G. (**2003**). A study of the limitations to spray dryer outlet performance. Drying Technology, v. 21, n. 1, p. 895-917.

[4] Maury, M., Murphy, K., Kumar, S., Shi, L. & Lee, G. (**2005**). Effect of process variables on the powder yield of spray dried trehalose on a laboratory spray-dryer. European journal of pharmaceutics and bio-pharmaceutics, v. 59, no. 3, p. 556-573.

[5] Zhou, X., Chen, S. & Yu, Z. (**2004**). Effect of spray drying parameters on the processing of fermentation liquor. Bio-systems Engineering, v. 88, n. 2, p. 193-199.

[6] Zhongua, W.U. & Mujumdar, A. S. (**2006**). A parametric study of spray drying of a solution in a pulsating high- temperature

turbulent flow. Drying Technology, v. 24, n. 6, p. 751-761.

[7] Chegini, G. R. & Ghobadian, B. (**2007**). Spray dryer parameters for fruit juice drying. World Journal of Agricultural Sciences, v. 3, n. 2, p. 230-236.

[8] Athanasia, M.G. & Konstantinos, G. A. (**2003)**. Influence of spray drying conditions on tomato powder moisture. Proceedings of 3rd International Symposium Food Rheology and Structure**,** p**.** 643-644.

[9] Phogpipatpong, M., Patamarajvichian, P., Namkhot, S. & Amomviriyakul, S. (**2008)**. Optimiztion of spray drying condition for longan drink powder using response surface methodology. Proceedings of International Workshop on Tropical and Subtropical Fruits ISHS Acta Horticulturae, p. 787.

[10] Prinn, K. B., Costantino, H.R. & Tracy, M. (**2002**). Statistical modeling of protein spray drying at the lab scale. AAPS Pharm SciTech, v. 3, n. 1, article-4.

[11] Goula, A. M. & Adamopoulos, K. G. (**2003**). Spray drying performance of a laboratory spray dryer for tomato powder preparation. Drying technology, v. 21, n. 7, p. 1273-1289.

[12] Lin, J.C. & Gentry, J.W. (**2003**). Spray drying drop morphology: Experimental study, Aerosol science and technology, v. 37, n. 1, p. 15-32.

[13] Iskandar, F., Gradon, L. & Okuyama, K. J. (**2003)**. Control of the morphology of nanostructured particles prepared by the spray drying of a nano-particle sol. Colloid and Interface Science, v. 265, n. 2, p. 296-303.

[14] Donhowe, D. P., Amundson, C. H. & Hill, C. G. (**1990**). Performance of heat recovery system for a spray dryer. Food Process Engineering, v. 12, n. 1, p. 13-32.

[15] Kent, J. & McLeod, J. (**2007**). Spray dryer optimisation. Powder/ Bulk Solids : The Source for Dry Processing and Bulk Handling Technology, February**.**

[16] Greenwald, C. G. & King, C. J. (**1982).** The *effects of drying conditions* on the properties of *spray*-dried particles. Food Process Engineering**, v.** 4, n. 3**, p. 171-187.**

[17] Bhandari, B. R., Datta, N., Crooks, R., Howes, T. & Rigby, S. (**1997**). A semi-empirical approach to optimise the quantity of drying aids required to spray dry sugar-rich foods. Drying Technology, v. 15, n. 10, p. 2509 — 2525.

[18] Zbiciński, I., Piatkowski, M. & Prajs, W. (**2005**). Determination of spray-drying kinetics in a small scale. Drying Technology: An International Journal, v. 23, n. 8, p. 1751 – 1759.

[19] Katarzyna, S., Dorota W.-R. & Gonçalves, A. (**2005**). Spray-drying of α-amylase—the effect of process variables on the enzyme inactivation. Drying Technology: An International Journal, v. 23, n. 4, p. 941 – 953.

[20] Chegini, G. R. & Ghobadian, B. (**2005**). Effect of spray-drying conditions on physical properties of orange juice powder. Drying Technology: An International Journal , v. 23, n. 3, p. 657– 668.

[21] Namaldi A., Çalik, P. & Uludag, Y. (**2006**). Effects of spray drying temperature and additives on the stability of serine alkaline protease powders. Drying Technology journal,v.24,n.11,p.1495–1500.

[22] Anandharamakrishnan, C., Rielly, D. & Stapley, A. G. F. (**2007**). Effects of Process Variables on the Denaturation of Whey Proteins during Spray Drying. Drying Technology: An International Journal, v. 25, n. 5, p. 799–807.

[23] William,V. (**1969**). Applied statistics for engineers. McGraw-Hill.

[24] Sahoo, A. & Roy, G. K. (**2007**). Artificial neural network approach to segregation characteristic of binary homogeneous mixtures in promoted gas solid fluidized beds. Power Technology, v. 17, n. 1, p. 54-62.

Table-1 : Scope of the experiment

Sl. No.	**Various Salts**	**Ms**	**Ti, °C**	**Uasp×10^3, Kg/cm^2**	**Up, ml/min**	**Cs, gm/ml**
1	$(NH_4)_2SO_4$	132.13	120	4.78	2.2796	0.1
2	Na_2SO_4	142.04	120	4.78	2.2796	0.1
3	NaCl	58.54	120	4.78	2.2796	0.1
4	$C_6H_{14}O_6$	182.17	120	4.78	2.2796	0.1
5	$(NH_4)_2SO_4$	132.13	140	4.78	2.2796	0.1
6	$(NH_4)_2SO_4$	132.13	160	4.78	2.2796	0.1
7	$(NH_4)_2SO_4$	132.13	180	4.78	2.2796	0.1
8	$(NH_4)_2SO_4$	132.13	120	9.23	2.2796	0.1
9	$(NH_4)_2SO_4$	132.13	120	13.0	2.2796	0.1
10	$(NH_4)_2SO_4$	132.13	120	17.0	2.2796	0.1
11	$(NH_4)_2SO_4$	132.13	120	4.78	3.2143	0.1
12	$(NH_4)_2SO_4$	132.13	120	4.78	3.9859	0.1
13	$(NH_4)_2SO_4$	132.13	120	4.78	5.3159	0.1
14	$(NH_4)_2SO_4$	132.13	120	4.78	2.2796	0.2
15	$(NH_4)_2SO_4$	132.13	120	4.78	2.2796	0.3
16	$(NH_4)_2SO_4$	132.13	120	4.78	2.2796	0.4
17	$(NH_4)_2SO_4$	132.13	120	4.78	2.2796	0.1
18	$(NH_4)_2SO_4$	132.13	120	4.78	2.2796	0.1
19	$(NH_4)_2SO_4$	132.13	120	4.78	2.2796	0.1

Table-2 (A): Comparison of calculated values of %yield for salt solution obtained from the dimensional analysis with the experimentally measured ones.

Sl. No	T_i ,°C	U_{asp}, kg/cm2	U_p, ml/min	C_s, gm/ml	P_{i-air}, kg/cm2	M_s	Exp-%Yield	Cal-%Yield	%dev.
1	120	0.00478	2.2796	0.1	2.1092	132.13	68.6	67.268	0.020
2	140	0.00478	2.2796	0.1	2.1092	132.13	65.8	65.697	0.002
3	160	0.00478	2.2796	0.1	2.1092	132.13	64.5	64.366	0.002
4	180	0.00478	2.2796	0.1	2.1092	132.13	63.5	63.214	0.004
5	120	0.00923	2.2796	0.1	2.1092	132.13	70.4	63.343	0.100
6	120	0.013	2.2796	0.1	2.1092	132.13	61.9	61.391	0.008
7	120	0.017	2.2796	0.1	2.1092	132.13	59.9	59.905	-8.8E-05
8	120	0.00478	3.2143	0.1	2.1092	132.13	60.54	53.524	0.116
9	120	0.00478	3.9859	0.1	2.1092	132.13	56.27	46.388	0.176
10	120	0.00478	5.3159	0.1	2.1092	132.13	32.9	38.303	-0.164
11	120	0.00478	2.2796	0.2	2.1092	132.13	69.9	70.416	-0.007
12	120	0.00478	2.2796	0.3	2.1092	132.13	71.26	72.325	-0.014
13	120	0.00478	2.2796	0.4	2.1092	132.13	78.14	73.711	0.057
14	120	0.00478	2.2796	0.1	2.8122	132.13	55.4	62.567	-0.129
15	120	0.00478	2.2796	0.1	3.5153	132.13	60.2	59.148	0.0174
16	120	0.00478	2.2796	0.1	4.2183	132.13	52.83	56.495	-0.069
17	120	0.00478	2.2796	0.1	2.1092	142.04	70.29	67.085	0.046
18	120	0.00478	2.2796	0.1	2.1092	58.54	64.85	69.358	-0.069
19	120	0.00478	2.2796	0.1	2.1092	182.17	57.18	66.461	-0.162

Table-2 (B), Comparison of the calculated outlet temperature with the experimental outlet temperature for salt solution by dimensional analysis

Sl. No	T_i ,°C	U_{asp}, kg/cm2	U_p, ml/min	C_s, gm/ml	P_{i-air}, kg/cm2	M_s	T_o –exp, °C	T_o- cal, °C	%dev.
1	120	0.00478	2.2796	0.1	2.1092	132.13	51.2	51.927	-1.421
2	140	0.00478	2.2796	0.1	2.1092	132.13	60.7	58.65	3.370
3	160	0.00478	2.2796	0.1	2.1092	132.13	68.2	65.181	4.425
4	180	0.00478	2.2796	0.1	2.1092	132.13	69.5	71.539	-2.934
5	120	0.00923	2.2796	0.1	2.1092	132.13	58.2	59.334	-1.949
6	120	0.013	2.2796	0.1	2.1092	132.13	61.4	63.598	-3.580
7	120	0.017	2.2796	0.1	2.1092	132.13	66.5	67.151	-0.979
8	120	0.00478	3.2143	0.1	2.1092	132.13	49.6	47.997	3.231
9	120	0.00478	3.9859	0.1	2.1092	132.13	46.4	45.689	1.531
10	120	0.00478	5.3159	0.1	2.1092	132.13	42.4	42.773	-0.880
11	120	0.00478	2.2796	0.2	2.1092	132.13	47.5	49.628	-4.480
12	120	0.00478	2.2796	0.3	2.1092	132.13	44.3	48.330	-9.098
13	120	0.00478	2.2796	0.4	2.1092	132.13	48.4	47.430	2.002
14	120	0.00478	2.2796	0.1	2.8122	132.13	48.1	49.637	-3.196
15	120	0.00478	2.2796	0.1	3.5153	132.13	45.2	47.930	-6.041
16	120	0.00478	2.2796	0.1	4.2183	132.13	46.7	46.580	0.257
17	120	0.00478	2.2796	0.1	2.1092	142.04	56.5	52.402	7.252
18	120	0.00478	2.2796	0.1	2.1092	58.54	49.4	46.869	5.123
19	120	0.00478	2.2796	0.1	2.1092	182.17	57.2	54.070	5.471

Table-3: Effects of variables for 2^{6-2} Fractional Factorial Design

Treatment Combination	Level of factor				Interactions										
	A	B	C	D	AB	AC	AD	BC	BD	CD	E=ABC	ABD	ACD	F=BCD	ABCD
I	-	-	-	-	+	+	+	+	+	+	-	-	-	-	+
A	+	-	-	-	-	-	-	+	+	+	+	+	+	-	-
B	-	+	-	-	-	+	+	-	-	+	+	+	-	+	-
Ab	+	+	-	-	+	-	-	-	-	+	-	-	+	+	+
C	-	-	+	-	+	-	+	-	+	-	+	-	+	+	-
Ac	+	-	+	-	-	+	-	-	+	-	-	+	-	+	+
Bc	-	+	+	-	-	-	+	+	-	-	-	+	+	-	+
Abc	+	+	+	-	+	+	-	+	-	-	+	-	-	-	-
D	-	-	-	+	+	+	-	+	-	-	-	+	+	+	-
Ad	+	-	-	+	-	-	+	+	-	-	+	-	-	+	+
Bd	-	+	-	+	-	+	-	-	+	-	+	-	+	-	+
Abd	+	+	-	+	+	-	+	-	+	-	-	+	-	-	-
Cd	-	-	+	+	+	-	-	-	-	+	+	+	-	-	+
Acd	+	-	+	+	-	+	+	-	-	+	-	-	+	-	-
Bcd	-	+	+	+	-	-	-	+	+	+	-	-	-	+	-
Abcd	+	+	+	+	+	+	+	+	+	+	+	+	+	+	+

Table-4: Calculation of outlet temperature of salt solution by fractional factorial design

T_i	U_{asp}	U_p	C_s	$P_{i\text{-}air}$	M_s	T_o Exp	A eff	Beff	Ceff	Deff
120	0.00478	2.2796	0.1	2.1092	132.13	51.2	-1	-1	-1	-1
180	0.00478	2.2796	0.1	2.1092	132.13	69.5	1	-1	-1	-1
120	0.00478	2.2796	0.1	2.1092	132.13	58.2	-1	1	-1	-1
180	0.00478	2.2796	0.1	2.1092	132.13	61.4	1	1	-1	-1
120	0.00923	2.2796	0.1	2.1092	132.13	49.6	-1	-1	1	-1
180	0.013	2.2796	0.1	2.1092	132.13	46.4	1	-1	1	-1
120	0.017	2.2796	0.1	2.1092	132.13	47.5	-1	1	1	-1
180	0.00478	3.2143	0.1	2.1092	132.13	44.3	1	1	1	-1
120	0.00478	3.9859	0.1	2.1092	132.13	48.1	-1	-1	-1	1
180	0.00478	5.3159	0.1	2.1092	132.13	45.2	1	-1	-1	1
120	0.00478	2.2796	0.2	2.1092	132.13	56.5	-1	1	-1	1
180	0.00478	2.2796	0.3	2.1092	132.13	49.4	1	1	-1	1
120	0.00478	2.2796	0.4	2.1092	132.13	66.5	-1	-1	1	1
180	0.00478	2.2796	0.1	2.8122	132.13	42.4	1	-1	1	1
120	0.00478	2.2796	0.1	3.5153	132.13	48.4	-1	1	1	1
180	0.00478	2.2796	0.1	4.2183	132.13	46.7	1	1	1	1
140	0.00478	2.2796	0.1	2.1092	142.04	60.7	-0.333	-1	-1	-1
160	0.00478	2.2796	0.1	2.1092	58.54	68.2	0.333	-1	-1	-1
120	0.00478	2.2796	0.1	2.1092	182.17	49.4	-1	-1	-1	-1
120	0.00478	2.2796	0.1	2.1092	132.13	57.2	-1	-1	-1	-1

Continuation of Table-4

Eeff	Feff	AB eff	AC eff	AD eff	BC eff	BD eff	CDeff	ABD eff	ACD eff	ABCDeff	T_o cal	%Dev
-1	-1	1	1	1	1	1	1	-1	-1	1	51.20	0
1	-1	-1	-1	-1	1	1	1	1	1	-1	69.50	-0.006
1	1	-1	1	1	-1	-1	1	1	-1	-1	58.20	0
-1	1	1	-1	-1	-1	-1	1	-1	1	1	61.42	-0.026
1	1	1	-1	1	-1	1	-1	-1	1	-1	49.61	-0.024
-1	1	-1	1	-1	-1	1	-1	1	-1	1	46.41	-0.026
-1	-1	-1	-1	1	1	-1	-1	1	1	1	47.51	-0.017
1	-1	1	1	-1	1	-1	-1	-1	-1	-1	44.31	-0.018
-1	1	1	1	-1	1	-1	-1	1	1	-1	48.11	-0.017
1	1	-1	-1	1	1	-1	-1	-1	-1	1	45.21	-0.027
1	-1	-1	1	-1	-1	1	-1	-1	1	1	56.49	0.014
-1	-1	1	-1	1	-1	1	-1	1	-1	-1	49.39	0.024
1	-1	1	-1	-1	-1	-1	1	1	-1	1	66.48	0.030
-1	-1	-1	1	1	-1	-1	1	-1	1	-1	42.40	-1.7E-14
-1	1	-1	-1	-1	1	1	1	-1	-1	-1	48.40	1.47E-14
1	1	1	1	1	1	1	1	1	1	1	46.72	-0.043
-1	0.19	0.333	0.333	0.333	1	1	1	-0.33	-0.33	0.333	53.83	11.305
-1	0.19	-0.33	-0.33	-0.33	1	1	1	0.333	0.333	-0.333	58.20	14.660
-1	-1	1	1	1	1	1	1	-1	-1	1	51.20	-3.644
-1	1	1	1	1	1	1	1	-1	-1	1	48.30	15.559

Table-5: Calculation of %Yield of salt solution by fractional factorial design.

T_i	U_{asp}	U_p	C_s	$P_{i\text{-}air}$	M_s	Y-exp	A eff	Beff	Ceff	Deff
120	0.00478	2.2796	0.1	2.1092	132.13	68.6	-1	-1	-1	-1
180	0.00478	2.2796	0.1	2.1092	132.13	63.5	1	-1	-1	-1
120	0.00478	2.2796	0.1	2.1092	132.13	70.4	-1	1	-1	-1
180	0.00478	2.2796	0.1	2.1092	132.13	61.9	1	1	-1	-1
120	0.00923	2.2796	0.1	2.1092	132.13	60.54	-1	-1	1	-1
180	0.013	2.2796	0.1	2.1092	132.13	56.27	1	-1	1	-1

120	0.017	2.2796	0.1	2.1092	132.13	69.9	-1	1	1	-1
180	0.00478	3.2143	0.1	2.1092	132.13	71.26	1	1	1	-1
120	0.00478	3.9859	0.1	2.1092	132.13	55.4	-1	-1	-1	1
180	0.00478	5.3159	0.1	2.1092	132.13	60.2	1	-1	-1	1
120	0.00478	2.2796	0.2	2.1092	132.13	70.29	-1	1	-1	1
180	0.00478	2.2796	0.3	2.1092	132.13	64.85	1	1	-1	1
120	0.00478	2.2796	0.4	2.1092	132.13	59.9	-1	-1	1	1
180	0.00478	2.2796	0.1	2.8122	132.13	32.9	1	-1	1	1
120	0.00478	2.2796	0.1	3.5153	132.13	78.14	-1	1	1	1
180	0.00478	2.2796	0.1	4.2183	132.13	52.83	1	1	1	1
140	0.00478	2.2796	0.1	2.1092	142.04	65.8	-0.33	-1	-1	-1
160	0.00478	2.2796	0.1	2.1092	58.54	64.5	0.333	-1	-1	-1
120	0.00478	2.2796	0.1	2.1092	182.17	57.18	-1	-1	-1	-1

Continuation of Table-5

Eeff	Feff	AB eff	AC eff	AD eff	BC eff	BD eff	CDeff	ABDeff	ACDeff	ABCDeff	Y-cal	%Dev
-1	-1	1	1	1	1	1	1	-1	-1	1	68.594	0.009
1	-1	-1	-1	-1	1	1	1	1	1	-1	63.502	-0.002
1	1	-1	1	1	-1	-1	1	1	-1	-1	70.416	-0.023
-1	1	1	-1	-1	-1	-1	1	-1	1	1	61.904	-0.006
1	1	1	-1	1	-1	1	-1	-1	1	-1	60.549	-0.015
-1	1	-1	1	-1	-1	1	-1	1	-1	1	56.257	0.024
-1	-1	-1	-1	1	1	-1	-1	1	1	1	69.911	-0.016
1	-1	1	1	-1	1	-1	-1	-1	-1	-1	71.239	0.030
-1	1	1	1	-1	1	-1	-1	1	1	-1	55.402	-0.003
1	1	-1	-1	1	1	-1	-1	-1	-1	1	60.189	0.018
1	-1	-1	1	-1	-1	1	-1	-1	1	1	70.284	0.009
-1	-1	1	-1	1	-1	1	-1	1	-1	-1	64.851	-0.002
1	-1	1	-1	-1	-1	-1	1	1	-1	1	59.897	0.006
-1	-1	-1	1	1	-1	-1	1	-1	1	-1	32.924	-0.073
-1	1	-1	-1	-1	1	1	1	-1	-1	-1	78.119	0.028
1	1	1	1	1	1	1	1	1	1	1	52.846	-0.030
-1	0.19	0.333	0.333	0.333	1.	1	1.	-0.33	-0.33	0.333	65.612	0.285
-1	0.19	-0.33	-0.33	-0.33	1.	1	1	0.333	0.333	-0.333	63.042	2.261
-1	1	1	1	1	1	1	1	-1	-1	1	67.904	-18.755

Table-6 : Comparisons of the outputs obtained by different methods

Items	Regression Analysis		Fractional Factorial design	
	%Yield, Y	Outlet Temp. (T_o)	%Yield, Y	Outlet Temp. (T_o)
Chi-square (ξ^2)	7.611486	1.739827	2.044807982	3.694234
Standard Deviation	0.088225	4.313751	4.365565	5.149021
Mean Deviation	-0.00369	0.120611	-0.85553	1.8872

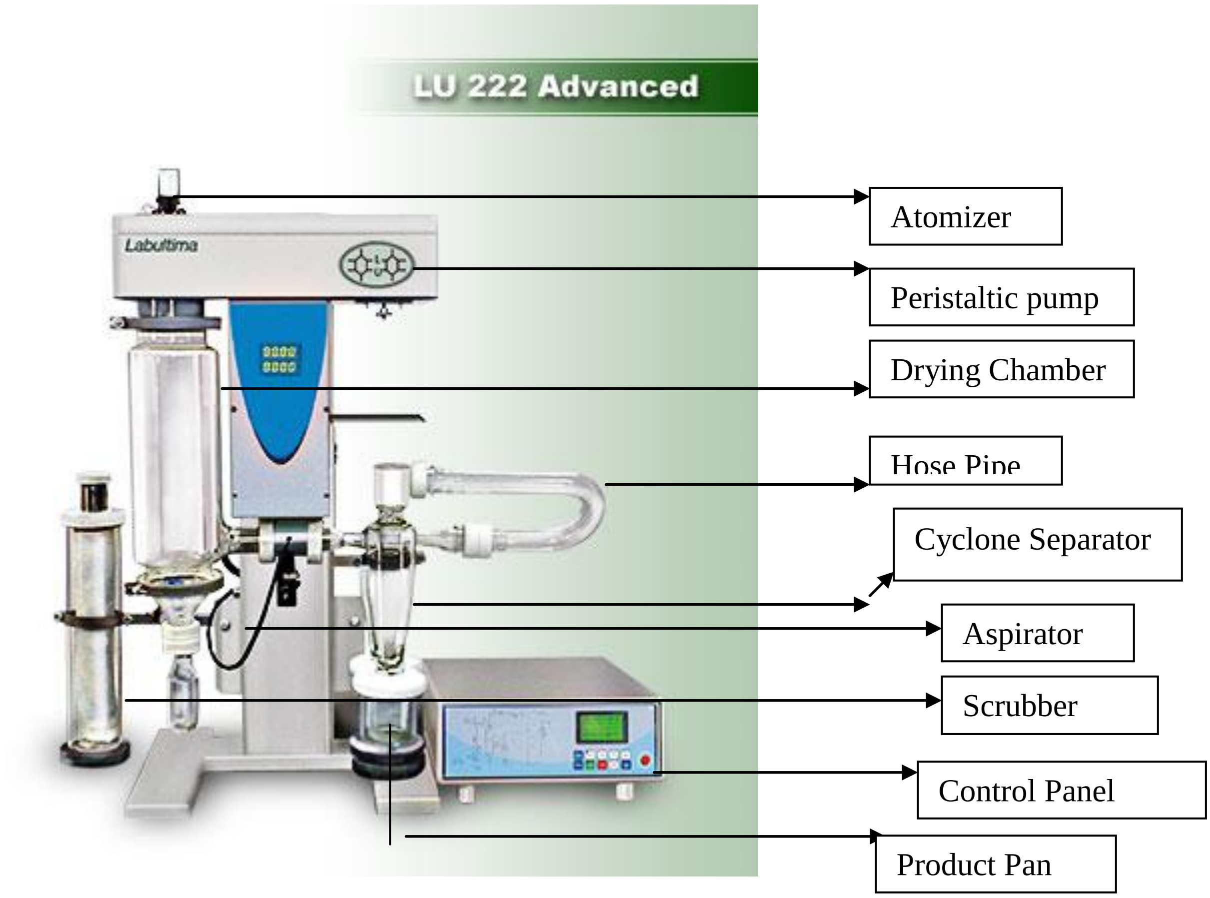

Figure-1: Experimental Set-up (Labultima Laboratory Spray Dryer)

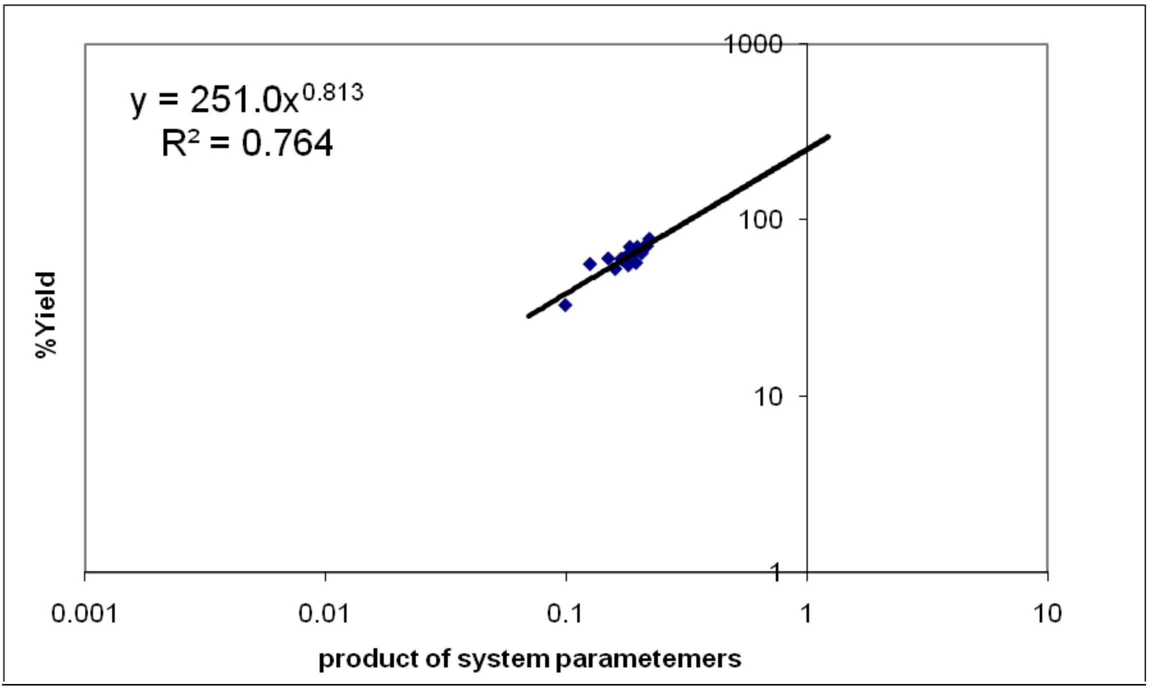

Figure-2(A) : Correlation plot for Percentage of Yield against the system parameters.

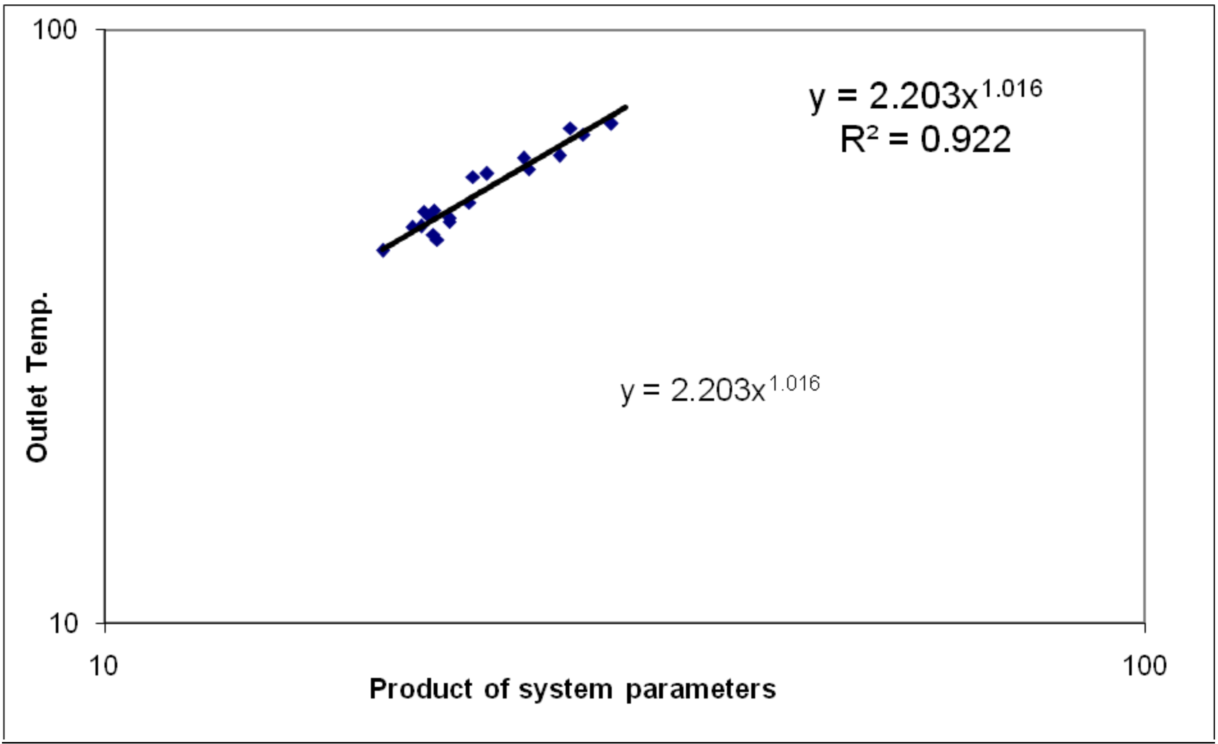

Figure-2(B) : Correlation plot for outlet temperature of salt solution against the system parameters

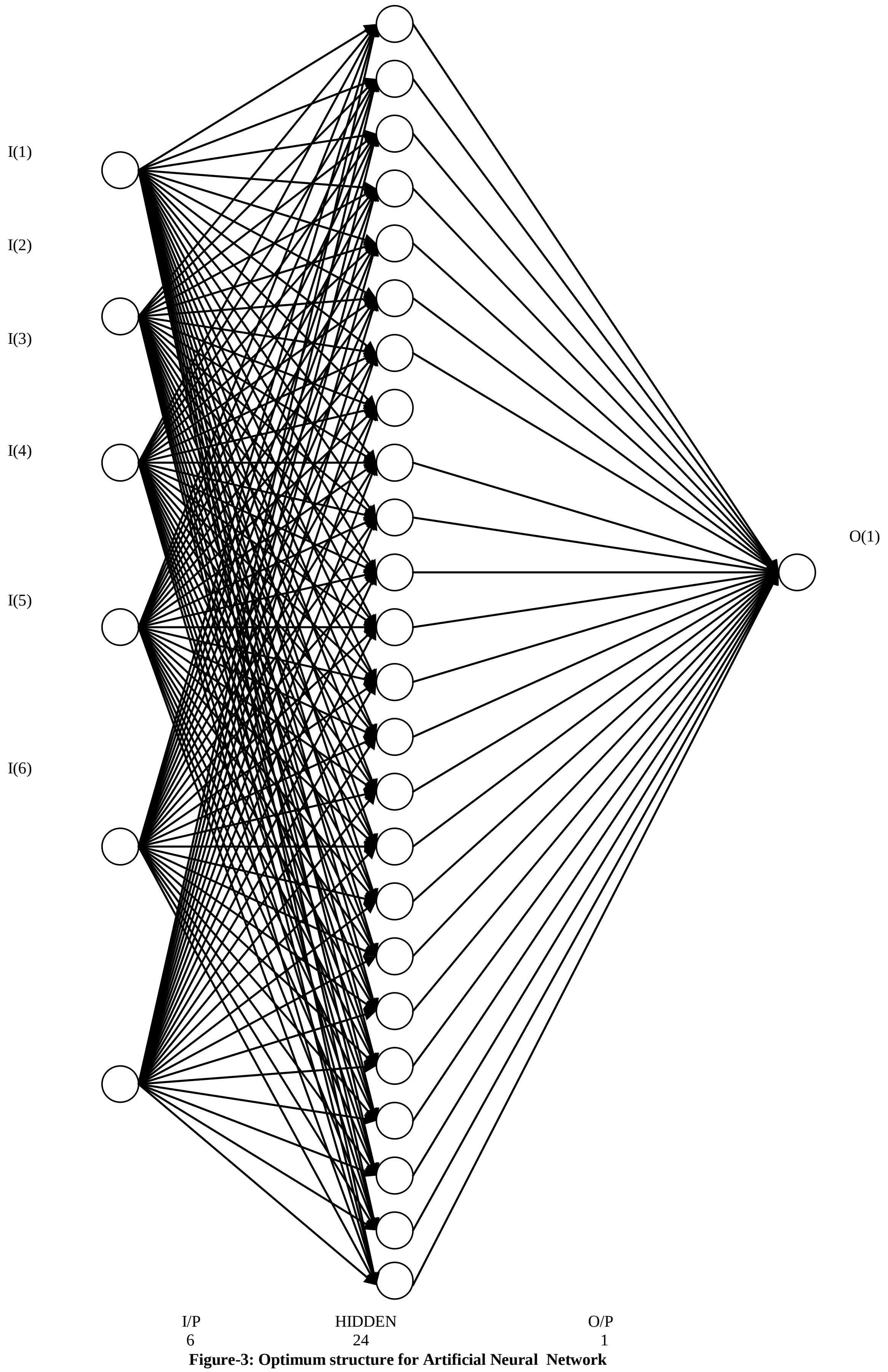

Figure-3: Optimum structure for Artificial Neural Network

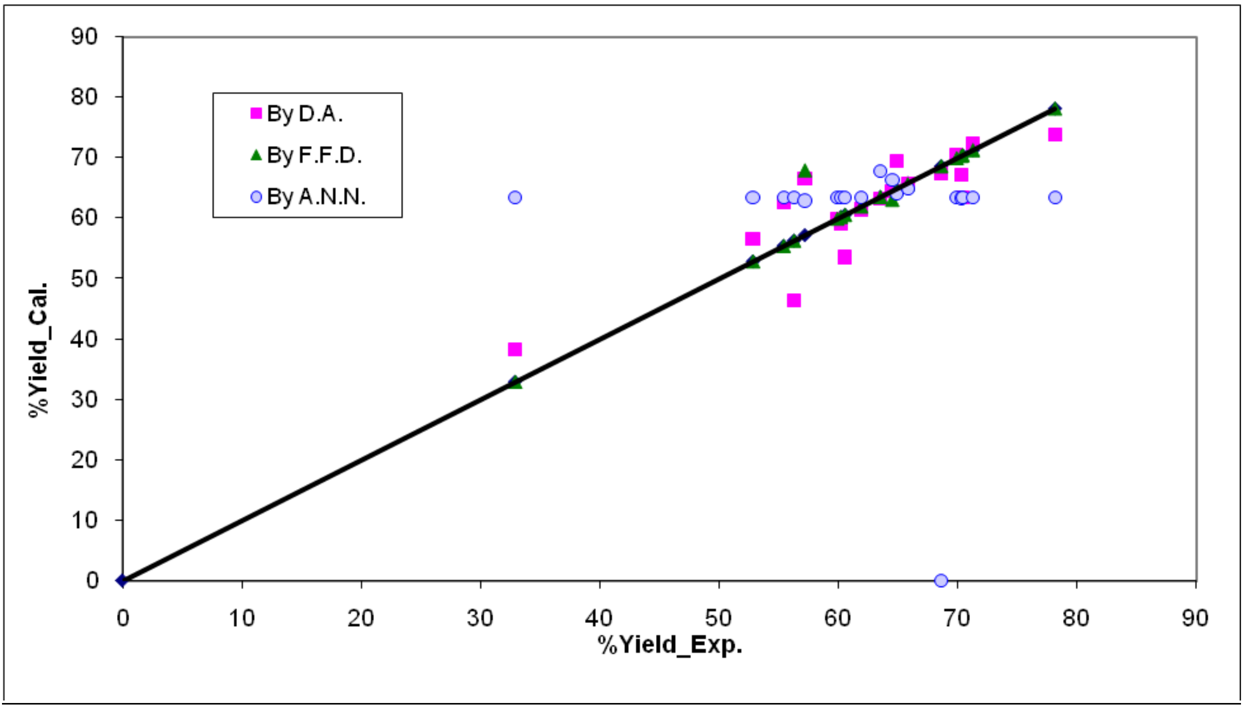

Figure-4(A) : Comparison plot for calculated values of percentage of Yield obtained by different methods against experimental values

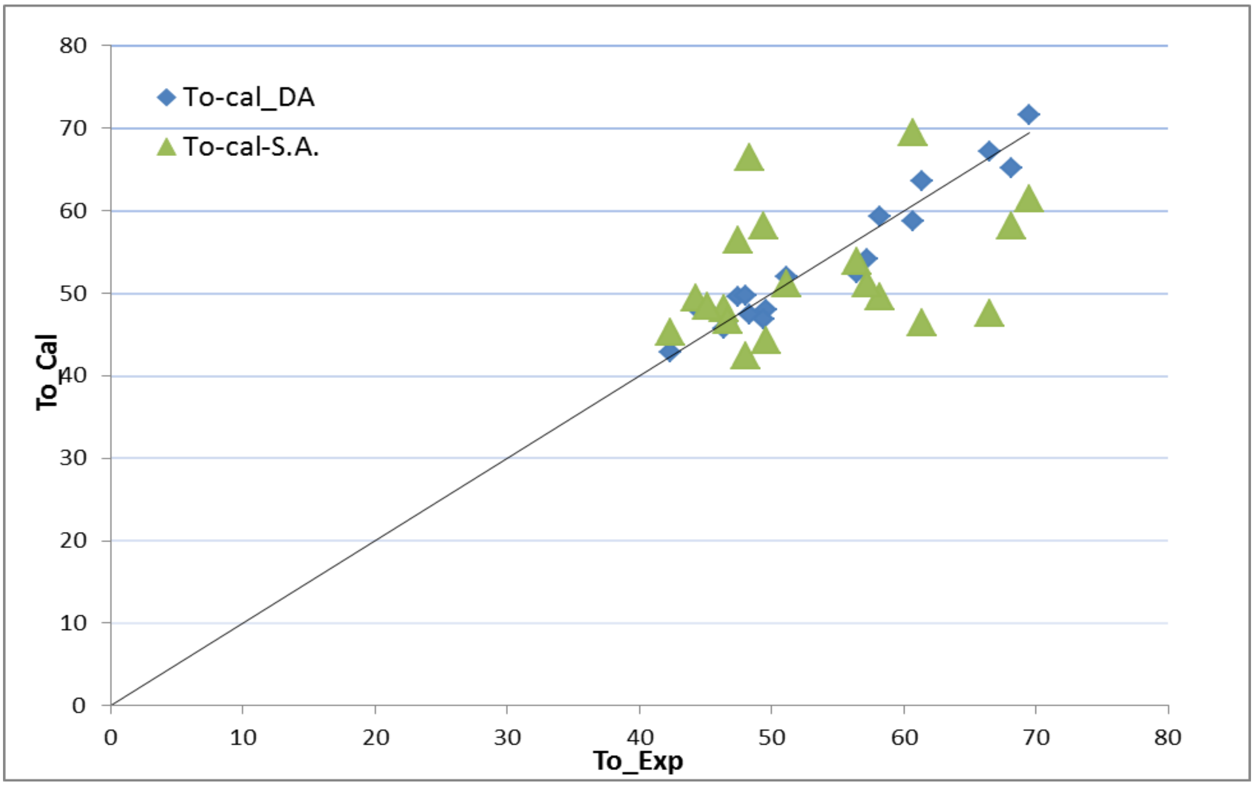

Figure-4(B) : Comparison plot for calculated values of outlet temperature of salt solution obtained by different methods against experimental values.

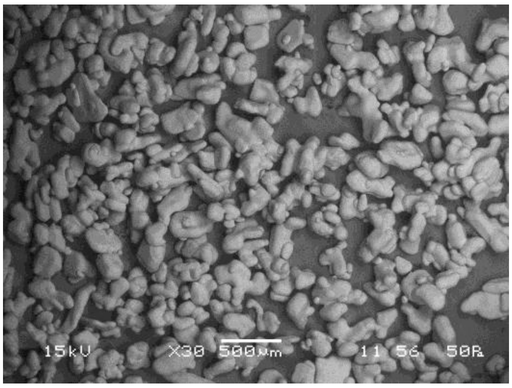

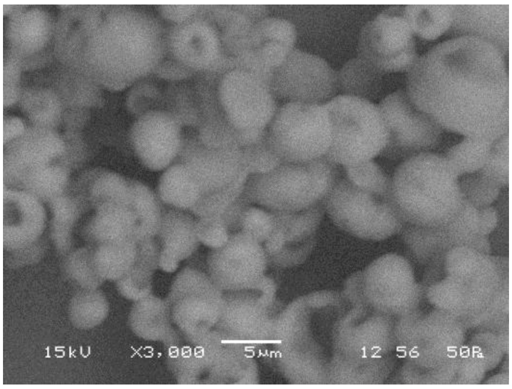

Ammonium sulfate before spray drying Ammonium sulfate after spray drying

(Spray dried Ammonium sulfate collected in the cyclone separator operated at Ti = 120 ^oC, Uasp = 0.00478 kg/cm^2, Up = 2.279604 ml/min, Cs = 1gm/ml, Piair = 2.10919 kg/cm^2)

Figure-5: S.E.M. picture of $(NH_4)_2SO_4$ before and after spray drying.

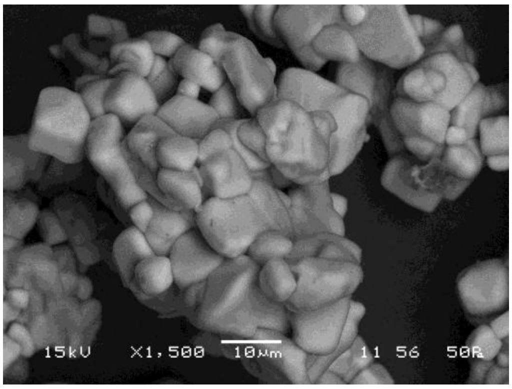

Sodium chloride before spray drying Sodium chloride after spray drying

(Spray dried mixture of NaCl collected in the cyclone separator operated at Ti= 120 ^oC, Uasp = 0.00478 kg/cm^2, Up= 2.279604 ml/min, Cs = 1gm/ml, Pi-air = 2.10919 kg/cm^2)

Figure-6 : S.E.M. picture of NaCl before and after spray drying.

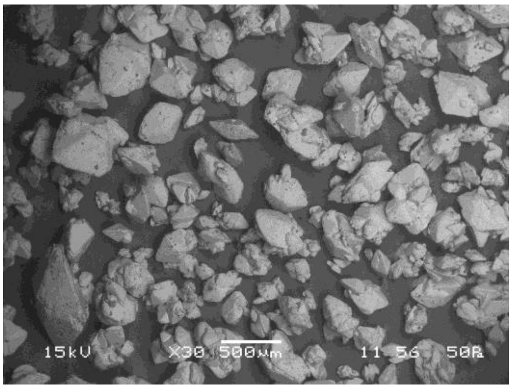

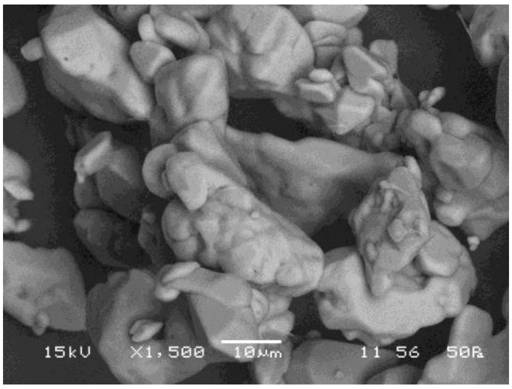

Sodium sulfate before spray drying Sodium sulfate after spray drying

(Spray dried mixture of Na_2SO_4 collected in the cyclone separator operated at Ti= 120 ^oC, Uasp = 0.00478 kg/cm^2, Up = 2.279604 ml/min, Cs = 1gm/ml, Pi-air = 2.10919 kg/cm^2)

Figure-7 : S.E.M. picture of Na_2SO_4 before and after spray drying

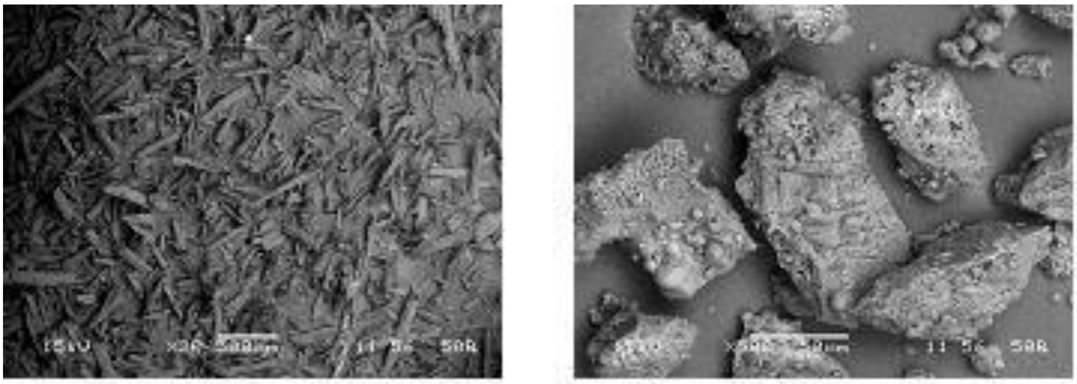

Mannitol before spray drying Mannitol after spray drying

(Spray dried mixture of Mannitol collected in the cyclone separator operated at Ti = 120 ^{o}C, Uasp = 0.00478 kg/cm^2, Up= 2.279604 ml/min, Cs= 1gm/ml, Pi-air = 2.10919 kg/cm^2)

Figure-8 : S.E.M. picture of $C_6H_{14}O_6$ before and after spray drying.